A Geochemical Model to Constrain Core-Mantle Equilibration During Large-Scale Impact-Driven Earth Accretion

Alexa Schultz

Advisor: Prof. Jun Korenaga

Second Reader: Assistant Prof. Alan Rooney

7 May 2024

A Senior Thesis presented to the faculty of the Department of Earth and Planetary Sciences, Yale University, in partial fulfillment of the Bachelor's Degree.

Contents

Abstract

Of the four terrestrial planets, Earth is unique in its capability to sustain life. There are many factors that determine a planet's habitability, but arguably the most important is the presence and cycling of volatiles. It is thought that these volatiles were delivered to Earth during planetary accretion and subsequently degassed from the interior to form Earth's atmosphere and oceans. To understand the emergence of life on Earth, then, we must first look at the accretion of planet Earth and how the materials delivered to Earth via large impactors interacted with the growing proto-Earth. Most models of Earth's accretion assume that the cores of impactors fully equilibrated with an entirely molten mantle, but this is unlikely, as it would require the impactor's core to fragment into very small pieces upon impact. In addition, it is not realistic for every impact to generate a full magma ocean. Here, I create a model for core accretion, using lead and tungsten as isotopic parameters to constrain degree of equilibration between the impactor core material, k_c, and the fraction of the Earth's mantle that is molten upon impact, k_m. I run this model for several possible cases of oxygen fugacity during accretion and compare the results. I discuss the sensitivity of core-mantle equilibration to multiple parameters including number of impactors, accretion timescale, and oxygen fugacity.

1. Introduction

The formation of planets in our solar system began 4.567 billion years ago with the condensation of solids from a protoplanetary disk surrounding our Sun, formed from the self-gravitational collapse of a molecular cloud. In the outer solar system, these solids were volatile-rich, as the lower temperatures of the protoplanetary disk facilitated condensation of ice and organics. In the inner solar system, where the disk temperature was higher, these solids were metals and silicates (Halliday and Canup, 2022). The metal and silicate solid grains of the early disk then aggregated to kilometer-sized planetesimals within a short timeframe during the first few million years of the solar system. These planetesimals collided due to gravity and gas drag during a fast period of runaway growth, which in turn formed larger planetary embryos (Morbidelli et al., 2012). Collisions between bodies during accretion and radioactive decay of isotopes caused planetary interiors to heat up and differentiate into a metal-silicate, or core-mantle, system in the early years of the solar system (Kleine et al., 2009). The rest of accretion for terrestrial planets was marched by stochastic collisions between these planetary embryos. Earth's accretion, in particular, is thought to have been bookended by an event in which a planetary embryo, Theia, collided with the proto-Earth to form the moon (Halliday and Canup, 2022). This is thought to be the last major event of Earth's accretion, marking the closing of the core and end of core formation (Rubie et al., 2015).

Earth's accretion and evolution is of particular interest to scientists studying planetary habitability due to its deviation from the paradigm of terrestrial planetary formation. According to this paradigm, temperatures in the inner-protoplanetary disk are much too high for volatile elements and compounds to condense and form the building blocks of terrestrial planets (Broadley et al., 2022). Still, volatiles such as hydrogen exist not only in liquid oceans on the

Earth's surface, but in silicate minerals in the crust, mantle, and even core (Peslier et al., 2017). Hydrogen and other volatiles likely could not have condensed directly from the protoplanetary disk and thus must have an exogenous origin. Extraterrestrial impactors are believed to have delivered such volatile elements to the Earth during core formation, during which their materials mixed with the molten mantle of a partial or full magma ocean caused by the energy of the impact (Deguen, et al., 2014). Constraining the extent to which these impactors equilibrated with the growing proto-Earth, then, is vital to understanding volatile accretion and evolution in terrestrial planets such as Earth and unraveling the process of making a habitable planet.

Many prior studies that have looked at Earth's accretion during the timeframe of core accretion have assumed complete equilibration of impactor cores with an entirely molten proto-Earth mantle. In these models, the embryo core sinks through a full magma ocean generated by the energy of the impact. As the embryo core sinks in the form of metal blobs, it fully equilibrates with the mantle around it, meaning the chemical signature of the original embryo's differentiation is fully erased. The problem with this model of core accretion is two-fold: firstly, the full core equilibration is only true if the core of the impactor fragments into exceedingly small pieces upon impact. Otherwise, larger pieces of the core do not fully equilibrate from the inside-out and thus retain the original composition of the embryo (Halliday, 2004). Secondly, it is highly unlikely that every giant impact generated a full magma ocean. Instead, depending on the conditions of the impact and the size of the colliding embryo, collisions likely generated partial magma oceans of varying proportions. In the case of a partial magma ocean, the impactor core would equilibrate only with the fraction of the mantle that is molten, and the remaining solid mantle would preserve its original chemical composition. These are vital considerations in evaluating core accretion and equilibration processes and understanding the early history of Earth. In this thesis, I create a geochemical model of impact-driven core formation to constrain the process of core-mantle equilibration. I calculate present-day isotopic ratios in Earth's mantle for two isotope systems based on this model, and use existing geochemical measurements of these isotopic ratios to place bounds on core-mantle equilibration. With my thesis, I aim to unravel the processes governing planetary formation and planetary accretion and explore the different conditions and parameters that affect core-mantle equilibration during impact-driven accretion.

2. Methods

2.1 Two-Stage Model

The simplest model of core formation is a two-stage model, where all of Earth's accretion occurs at a singular moment t_1. In this model, planetary embryos differentiate at $t = 0$, the time of solar system formation, and have the same bulk composition. From the differentiation of the embryos to the moment of accretion, the core-mantle system is closed in all embryos and there is no material exchange between the two reservoirs. At t_1, the embryos join instantaneously to form the Earth. The embryo mantles directly combine and mix, as in Figure 1b. A fraction of each embryo's core, k_c, equilibrates with the mantle as it sinks to the button. The rest of the embryo cores directly combine and do not equilibrate with the mantle (Figure 1a). This model only considers a full magma ocean, and does not consider differences in embryo composition, varying degree of equilibration between each embryo or a changing partition coefficient throughout accretion. Instead, this model was intended to constrain broad bounds on accretion and provide footing for the multi-stage model.

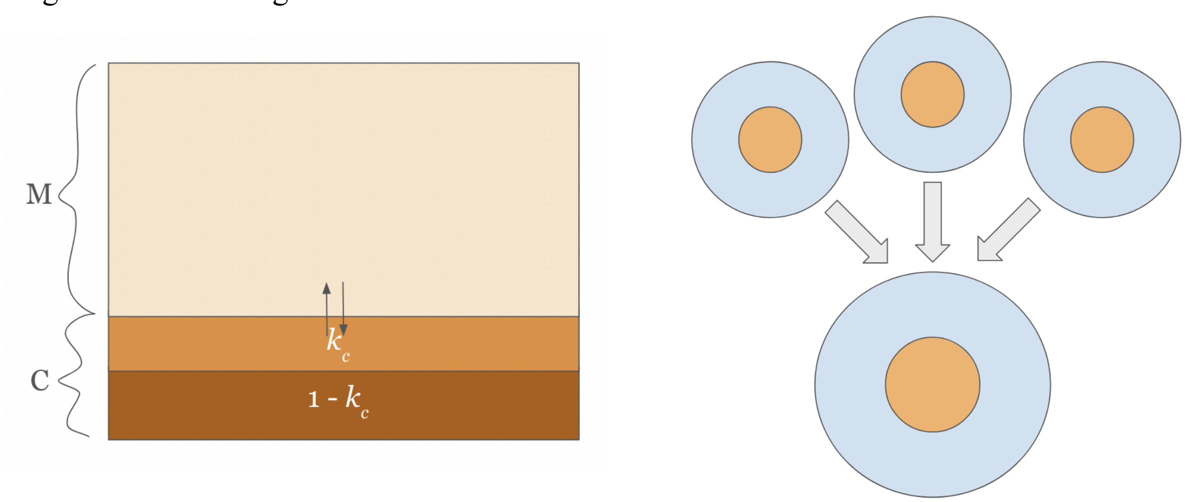

Figure 1. Two-stage model. a) k_c equilibrates with the mantle, while 1-k_c does not. **b)** Impactors join together instantaneously at t_1.

2.1.1 Two-stage model calculations

The embryos are in metal-silicate equilibrium at $t = 0$. The mantle and core of the embryos do not interact with each other and I assume no material exchange between the two. At the end of this period of equilibrium, we can express the concentrations of the daughter isotope d and the parent isotope p in the mantle as

$$d_{t_1}^m = d_0^m + p_0^m(1 - e^{-\lambda t_1}) \tag{1}$$

$$p_{t_1}^m = p_0^m(e^{-\lambda t_1}) \tag{2}$$

and the concentrations in the core as

$$\begin{aligned} d_{t_1}^c &= d_0^c \\ p_{t_1}^c &= 0 \end{aligned} \tag{3}$$

since the parent isotope in both systems is lithophile and does not go into the core.

At t_1, the embryos join to form the Earth and are no longer in equilibrium. If only a fraction k_c of the core equilibrates with the whole mantle, we can relate the time right before mixing t_1, and the time right after mixing, t'_1, through mass balance. Then,

$$k_c M_c d_{t_1}^c + M_m d_{t_1}^m = k_c M_c d_{t'_1}^c + M_m d_{t'_1}^m \tag{4}$$

where M_m is the mass of the mantle and M_c is the mass of the core. If F is the mass fraction of Earth's core, and M is the mass of the Earth, then

$$M_c = FM; M_m = (1 - F)M \tag{5}$$

and the prior mass balance equation can be rewritten as

$$k_c F d_{t_1}^c + (1 - F) d_{t_1}^m = k_c F d_{t'_1}^c + (1 - F) d_{t'_1}^m \tag{6}$$

Considering elemental partitioning, where partition coefficient $D = \frac{d^c}{d^m}$,

$$d_{t'_1}^c = D d_{t'_1}^m \tag{7}$$

$$d_{t_1}^c = d_0^c = D d_0^m \tag{8}$$

Using these relations and equation (2), we can rewrite equation (8) as

$$k_c F D d_0^m + (1-F)(d_0^m + p_0^m(1-e^{-\lambda t_1})) = k_c F D d_{t_1'}^m + (1-F) d_{t_1'}^m \quad (9)$$

We can solve the above equation for $d_{t_1'}^m$:

$$d_{t_1'}^m = d_0^m + (\frac{1-F}{k_c F D + (1-F)}) p_0^m (1-e^{-\lambda t_1}) \quad (10)$$

After mixing at t_1, the core-mantle system closes and there is no more isotopic exchange. Because the parent isotope is lithophile and does not partition to the core, the concentration of the parent isotope remains the same before and after mixing. We can write the concentration of the daughter isotope in the mantle at present day $t = 4567$ Myr as

$$d_t^m = d_{t_1'}^m + p_{t_1}^m (1-e^{-\lambda(t-t_1)}) \quad (11)$$

which can be written as

$$d_t^m = d_0^m + (\frac{1-F}{k_c F D + (1-F)}) p_0^m (1-e^{-\lambda t_1}) + p_{t_1}^m (1-e^{-\lambda(t-t_1)}) \quad (12)$$

We do not have exact concentration values for these isotopes, but we do have the isotopic ratios of the parent and daughter isotopes to a stable reference isotope c.

$$(\frac{d}{c})_t^m = (\frac{d}{c})_0^m + (\frac{1-F}{kFD + (1-F)})(\frac{p}{c})_0^m (1-e^{-\lambda t_1}) + (\frac{p}{c})_{t_1}^m (1-e^{-\lambda(t-t_1)}) \quad (13)$$

2.2 Multi-stage model

The two-stage model only provides broad bounds on the end time of core formation and the average fraction of impactor cores that equilibrate with the proto-Earth's mantle. A more accurate model is a multi-stage model, where there are multiple impacts throughout the timeframe of core accretion. This model takes into account both k_c, the fraction of the impactor core that equilibrates with the mantle, and k_m, the fraction of the mantle that is molten. The fraction k_c of the core only equilibrates with the fraction k_m of the mantle that is molten; the non-molten fraction of the mantle, 1-k_m, keeps the pre-impact mantle isotope composition. This model also incorporates a changing partition coefficient, because the partitioning of elements between metal and silicate phases is highly dependent on pressure, temperature, and oxygen fugacity conditions at the time and location of equilibration.

2.2.1 Multi-stage model calculations

We can derive an equation for the concentration of the daughter isotope in the mantle after a large-scale impact. At the time of impact, a certain fraction of the proto-Earth's mantle k_m becomes molten due to the energy of the impact. A fraction of the impactor's core k_c equilibrates with the molten portion of the mantle, while the remaining fraction 1-k_c is added directly to the proto-Earth's core without interacting with the mantle (Figure 2). The non-molten fraction of the mantle, 1-k_m, keeps the pre-impact mantle isotope composition.

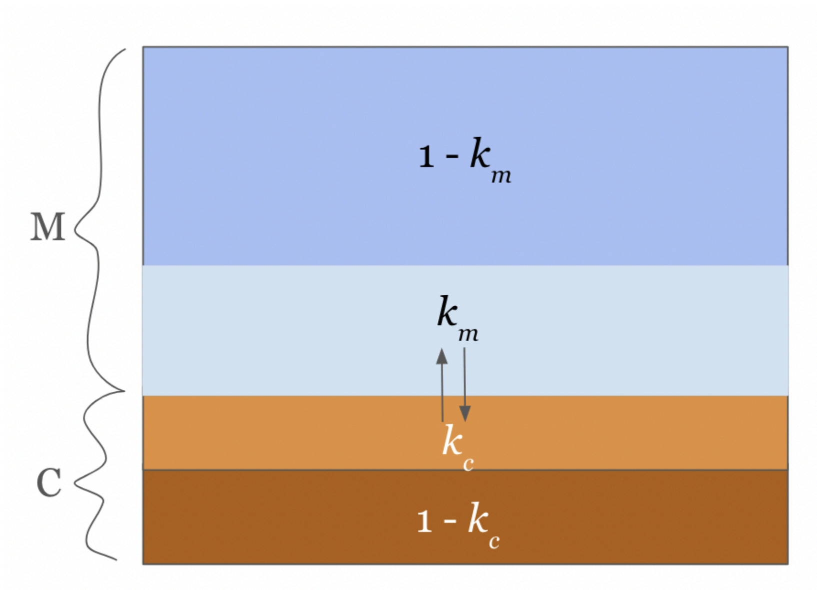

Figure 2. Simplified figure of multi-stage mixing. Mantle (blue) and core (orange) during equilibration. A fraction of the impactor core, k_c, equilibrates with the molten fraction of the mantle, k_m. The rest of the core and mantle do not equilibrate.

We can relate the composition of the mantle and core directly before mixing, denoted by d, and the composition of the mantle and core after mixing, denoted by d'. By mass conservation, we get this equation:

$$k_m M_m d_m + M_{IM} d_{IM} + k_c M_{IC} d_{IC} = (k_m M_m + M_{IM}) d'_m + k_c M_{IC} d'_{IC} \quad (14)$$

where M_{IM} is the mass of the impactor mantle and M_{IC} is the mass of the impactor core. During the impact, part of the impactor core and part of the new mantle are assumed to be in equilibrium, $d'_{IC} = Dd'_m$. Using that relation, $M_{IM} = (I - F)M_I$ and $M_{IC} = FM_I$ and the mass fraction relations used in the two-stage model, we can then rewrite the above equation as

$$(1-F)Mk_m d_m + (1-F)M_I d_{IM} + FM_I k_c d_{IC} \quad (15)$$
$$= (1-F)(M+M_I)k_m d'_m + FM_I k_c D d'_m$$

Combining the d'_m terms,

$$(1-F)Mk_m d_m + (1-F)M_I d_{IM} + k_c F M_I d_{IC} \quad (16)$$
$$= [k_m((1-F)Mk_m + (1-F)M_I + k_c FDM_I] d'_m$$

Thus,

$$d'_m = \frac{k_m((1-F)Md_m + (1-F)M_I d_{IM} + k_c F M_I d_{IC}}{k_m((1-F)M + (1-F)M_I) + k_c FDM_I} \quad (17)$$

This is only applicable to the portion of the mantle that is molten, k_m, so we average d'_m for that portion and d_m for 1-k_m to find the average isotopic concentration for the whole mantle,

$$(M_m + M_{IM})d''_m = (1-F)(M_m d_m + M_{IM} d_{IM}) + k_m (M_m + M_{IM}) d'_m \quad (18)$$

Using prior defined relations for the mass, and canceling out common terms, we can rewrite this as

$$d"_m = \frac{(1-k_m)(Md_m + M_I d_{IM}) + k_m(M+M_I)d'_m}{M+M_I} \tag{19}$$

We can generalize to a multistage model, where there are *i* number of impacts. M, the mass of the Earth, can be written as M_{i-1}, the mass of the Earth after the prior impact; this is because in the mass balance equation, M is equivalent to the mass of the proto-Earth before the addition of the impactor mass. M_I, the mass of the impactor, can then be written as ΔM_i, the change in mass of the Earth from after the prior impact to after the current impact. We also divide by the stable reference isotope, *c*, to get our model in terms of isotopic ratios.

$$(\frac{d}{c})_i^m = (\frac{d}{c})_{i-1}^{m"} + (\frac{p}{c})_{i-1}^m (1 - e^{-\lambda(t_i - t_{i-1})}) \tag{20}$$

$$(\frac{d}{c})_i^{m'} = \frac{(1-F)M_{i-1}k_i^m(\frac{d}{c})_i^m + (1-F)\Delta M_i(\frac{d}{c})_i^{IM} + k_i^c F\Delta M_i(\frac{d}{c})_i^{IC}}{(1-F)M_{i-1}k_i^m + (1-F)\Delta M_i + k_i^c FD\Delta M_i} \tag{21}$$

$$(\frac{d}{c})_i^{m"} = \frac{(1-k_i^m)(M_{i-1}(\frac{d}{c})_i^m + \Delta M_i(\frac{d}{c})_i^{IM}) + k_i^m(M_{i-1}+\Delta M_i)(\frac{d}{c})_i^{m'}}{M_{i-1}+\Delta M_i} \tag{22}$$

In this multi-stage mixing model, $(\frac{d}{c})_i^m$ is the isotopic ratio of the daughter isotope in the Earth's mantle directly before an i^{th} impact. This is equivalent to the ratio of the daughter isotope in the Earth's mantle directly after the prior (*i* - 1) impact and subsequent mixing plus the ratio of the additional daughter isotope produced from radioactive decay between the prior impact and the current one. When *i* = 1, $(\frac{d}{c})_{i-1}^m$ and $(\frac{p}{c})_{i-1}^m$ are equivalent to the initial daughter and parent isotopic ratios of the Earth at *t* = 0.

Because the impactors differentiated at *t* = 0 and have not experienced impacts themselves, the daughter isotope ratio within the impactor mantle, $(\frac{d}{c})_i^{IM}$, is defined as the initial ratio in the mantle plus the ratio corresponding to the excess daughter isotope that has been produced via decay of the parent isotope. The daughter isotope ratio within the impactor core, , $(\frac{d}{c})_i^{IC}$ remains constant at the initial ratio.

2.3 Accretion curve model

In order to determine the mass of the growing proto-Earth over the timescale of accretion, I use a simple exponential accretion model from Rudge et al. (2010),

$$M(t) = 1 - exp^{(-t/\tau_a)} \tag{23}$$

where τ_a is the mean age of accretion, or the time at which 63% of the Earth's mass has been accreted. I assume that at $M(t) = 0.90$, a final lunar-forming impact occurred, providing the last 10% of Earth's mass. Using a predetermined input value of τ_a, I first solve for the time *t* where $M(t) = 0.90$. I divide 0.90 by a predetermined number of impactors excluding the final lunar-forming impact, n_i, to calculate the mass of each impactor, which I keep constant for simplicity. I solve the accretion equation for the corresponding time of impact for each impactor, and then calculate the corresponding $M(t)$ value. Finally, I add a final impactor that adds the final 10% of Earth's mass. Figure 3 shows an example of an accretion curve for τ_a = 40 Myr and n_i = 14.

2.4 Partition coefficient parametrization

The partition coefficient *D* of an element is a measure of how that element is distributed between the Fe-rich metallic phase (core) and the silicate mantle. The partition coefficient of a specific element is a function of the temperature, pressure, and oxygen fugacity under which metal/silicate equilibration takes place; while the current partition coefficients of lead and tungsten are approximately 13 and 32 respectively, they were likely several orders of magnitude larger at the start of accretion.

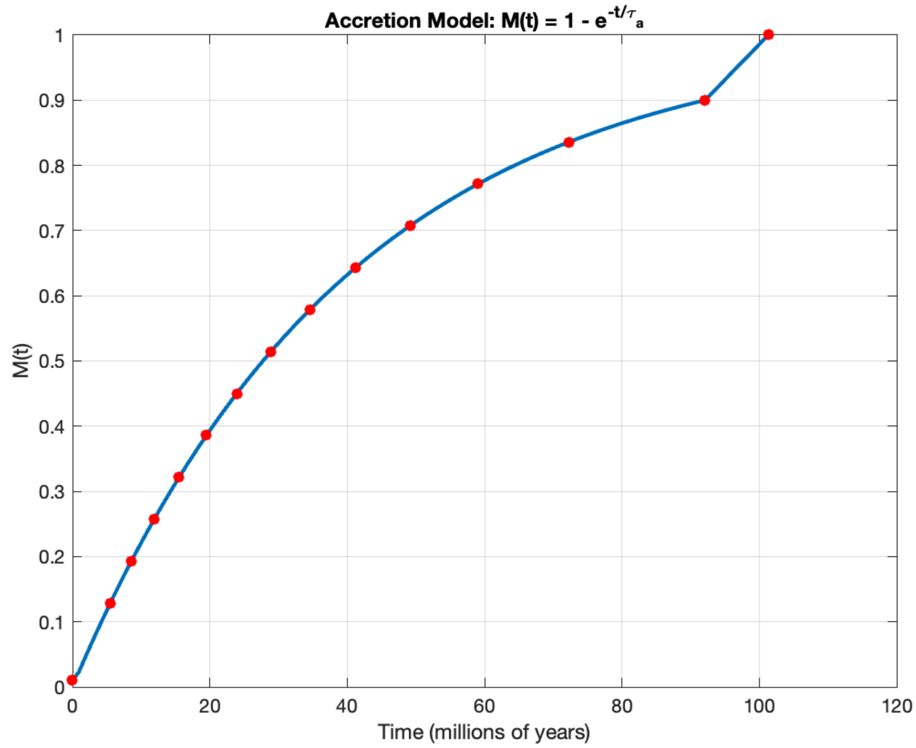

Figure 3. An accretion curve for τ_a = 40 Myr and n_i = 14, where n_i is the number of impactors excluding the lunar forming impactor. The red dots represent each impactor.

Per Rudge et al. (2010), we can write the partition coefficient of an element in as

$$\log_{10} D = a + b\frac{1}{T} + c\frac{P}{T} + dN - \frac{v}{4}\Delta IW - \frac{T_0}{T}\log_{10}\gamma_M^{met}(T_0) + \frac{v}{2}\log_{10}\gamma_{FeO}^{sil} \quad (23)$$

where *a*, *b*, *c*, and *d* are coefficients from experimental data, *v* is the assumed valence, and $\gamma_M^{met}(T_0)$ is the activity of elements in the metal phase at that reference temperature. These are all assumed constant for each element and given in Table 1. For all elements, T_0 is a reference temperature of 1873 K; γ_{FeO}^{sil} is the activity of FeO in the silicate, assumed to be 3; *N* is the molar ratio of non-bridging oxygens to tetrahedral cations in silicate melt, assumed to be 2.7. We must then write equations for *T* (temperature), *P* (pressure), and ΔIW (oxygen fugacity).

First, we define pressure as a function of $M(t)$,

$$P(t) = P_0 M(t)^{\frac{2}{3}} \text{in GPA} \tag{24}$$

where P_0 is a constant that represents the average pressure at the base of a magma ocean. I use a value of 44 GPa, which is approximately 33% of the current pressure at the core-mantle boundary.

Metal-silicate equilibration is assumed to take place on the peridotite liquidus, which can be written as

$$T(t) = 1973 + 28.57P(t) \text{ in K} \tag{25}$$

Oxygen fugacity (written here as ΔIW, the oxygen fugacity relative to the IW buffer in $\log_{10}$ units) evolves as the planet accretes. This can be written in terms of the initial oxygen fugacity, ΔIW_1, and the final oxygen fugacity, ΔIW_2. For the first 10% of accretion ($0 < M(t) < 0.1$), oxygen fugacity remains constant:

$$\Delta IW = \Delta IW_1$$

For the remaining 90% of accretion, oxygen fugacity increases linearly as

$$\Delta IW = \Delta IW_1 + (\Delta IW_2 - \Delta IW_1)\frac{M(t) - 0.1}{0.9} \tag{26}$$

Table 1. Constants used in partition coefficient parametrization, from Rudge et al. (2010), Supplementary Table 4.

Element	*v*	*a*	*b* (K)	*c* ($KGPa^{-1}$)	*d*	$\gamma_M^{met}(T_0)$
Pb	2	0.788	-2436	0	0	1.000
W	4.52	3.2	-1605	-115	0	0.9411

2.5 Isotopic decay

2.5.1 U–Pb system parameters

The uranium–lead isotope system is one of the most well-studied radioactive dating schemes in geology. Uranium-238 and uranium-235 are radioactive isotopes that decay into lead-206 and lead-207, respectively, through a series of alpha and beta decays, during which an alpha or beta particle ejects from the nucleus (Corfu, 2013). Uranium is a lithophile element, meaning it preferentially stays in the silicate phase (or mantle, in the case of the core-mantle system), while lead is siderophile and partitions to the metal phase (core). U/Pb ratios are not well constrained (Yin and Jacobsen, 2006). In the U-Pb system, ^{204}Pb is used as a stable reference isotope whose concentration does not change over time due to decay.

The bulk lead ratios at the time of solar system formation were measured from the Canyon Diablo meteorite in Arizona. Geochemical investigation of this iron meteorite revealed that it was of primary composition and represented the original bulk lead composition of the solar system (Patterson, 1956). I use these measured lead isotopic ratios and other values mentioned in Table 2 as inputs for my calculations. In addition, I take two prior studies and use their present day ($^{238}U/^{204}Pb$) mantle ratio to back-calculate the initial ($^{238}U/^{204}Pb$) mantle ratio, which I then use in my calculations. I use the other values from those studies, written in Table 3, as lower and upper bounds in the calculations. To calculate an initial ($^{235}U/^{204}Pb$) ratio, I use the ($^{235}U/^{238}U$) ratio in Table 2 to convert the initial ^{238}U ratio to a ^{235}U ratio.

Table 2. Input parameters for the U–Pb system, from Rudge et al. (2010), Supplementary Table 2

Parameter	Value	Remarks
λ_{238}	1.555×10^{-10} yr^{-1}	Decay constant of ^{238}U
λ_{235}	9.849×10^{-10} yr^{-1}	Decay constant of ^{235}U
$(^{235}\mathrm{U}/^{238}\mathrm{U})^{\mathrm{b}}_{\mathrm{t}}$	1/137.88	Present day value
$(^{206}\mathrm{Pb}/^{204}\mathrm{Pb})^{\mathrm{b}}_{0}$	10.294	Initial bulk value
$(^{207}\mathrm{Pb}/^{204}\mathrm{Pb})^{\mathrm{b}}_{0}$	10.294	Initial bulk value

Table 3. Constraints on present day lead and uranium isotopic ratios from experimental studies, from Rudge et al. (2010), Supplementary Table 3.

Reference	$(^{206}\mathrm{Pb}/^{204}\mathrm{Pb})^{\mathrm{m}}_{\mathrm{t}}$	$(^{207}\mathrm{Pb}/^{204}\mathrm{Pb})^{\mathrm{m}}_{\mathrm{t}}$	$(^{238}\mathrm{U}/^{204}\mathrm{Pb})^{\mathrm{m}}_{\mathrm{t}}$
Kwon et al. 1989	17.822	14.445	8.38
Allègre et al. 1998	18.400	15.565	9.12

2.5.2 Hf–W system parameters

Hafnium-tungsten is a short-lived isotope system in which hafnium-182 decays to tungsten-182. It is most often used to date processes related to the very early solar system due to its half-life of 8.9 ± 0.1 Myr. The system's ability to date processes within the first 60 Myr of solar system formation is particularly useful when studying terrestrial planet core formation. Hafnium and tungsten are both refractory elements, meaning they condense at high temperatures and thus are assumed to have been abundant in the hot inner protoplanetary disk building blocks (Kleine at al., 2009). Hafnium is a lithophile element, while tungsten is moderately siderophile, making the system a useful tracer for core-related processes. Both of these properties make the

Hf–W system most suitable for dating core formation (Lee and Halliday, 1995). In this system, ^{184}W is used as the stable reference isotope in isotopic ratios.

Most input parameters for the Hf–W system, such as the values in Table 3, are measured directly from meteorites and terrestrial samples or calculated on an isochron. Because hafnium-182 is a long extinct isotope, the initial (^{182}Hf/^{184}W) ratio of the mantle cannot be measured directly from samples. Instead, as in Lee and Halliday (1995), it is calculated suing the stable (^{180}Hf/^{184}W) ratio of the mantle and the initial (^{182}Hf/^{180}Hf) ratio of the bulk Earth:

$$\left(\frac{^{182}\mathrm{Hf}}{^{184}\mathrm{W}}\right)_0^{\mathrm{m}} = \left(\frac{^{180}\mathrm{Hf}}{^{184}\mathrm{W}}\right)^{\mathrm{m}} \times \left(\frac{^{182}\mathrm{Hf}}{^{180}\mathrm{Hf}}\right)_0^{\mathrm{b}} \tag{27}$$

Likewise, the initial ($^{182}W/^{184}W$) ratio of the mantle can be calculated as:

$$\left(\frac{^{182}\mathrm{W}}{^{184}\mathrm{W}}\right)_0^{\mathrm{m}} = \left(\frac{^{182}\mathrm{Hf}}{^{184}\mathrm{W}}\right)_0^{\mathrm{b}} = \left(\frac{^{182}\mathrm{Hf}}{^{184}\mathrm{W}}\right)_{\mathrm{t}}^{\mathrm{b}} - \left(\frac{^{180}\mathrm{Hf}}{^{184}\mathrm{W}}\right)_{\mathrm{t}}^{\mathrm{b}} \times \left(\frac{^{182}\mathrm{Hf}}{^{180}\mathrm{Hf}}\right)_0^{\mathrm{b}} \tag{28}$$

Because exact present day tungsten ratios in the mantle and bulk Earth are not well constrained, it is better to use the relative difference between the mantle tungsten ratio values and the chondritic tungsten ratio values, written as $\epsilon^{182}\mathrm{W}$.

Table 4. Input parameters for the Hf–W system from Rudge et al. (2010), Supplementary Table 1

Parameter	Value	Remarks
$\lambda_{^{182}\mathrm{Hf}}$	7.78×10^{-8} yr^{-1}	Decay constant of ^{182}Hf
$(^{182}\mathrm{Hf}/^{180}\mathrm{Hf})_0^{\mathrm{b}}$	9.72×10^{-5}	Initial bulk value
$(^{180}\mathrm{Hf}/^{184}\mathrm{W})_{\mathrm{t}}^{\mathrm{b}}$	1.23 ± 0.15	Present day bulk value
$(^{180}\mathrm{Hf}/^{184}\mathrm{Hf})_{\mathrm{t}}^{\mathrm{m}}$	20.06 ± 5.90	Present day mantle value
$\epsilon^{182}\mathrm{W}_{\mathrm{t}}$	1.9 ± 0.1	Present day value

3. Results

In this section, I report model results for three oxygen fugacity scenarios. I ran the model for several values of τ_a and n_i: values of τ_a ranged from 25 Myr to 170 Myr, and values of n_i were 10, 25, and 40. Based on these input parameters, the model calculates present-day isotopic ratios for lead and tungsten as a function of both k_m and k_c. I then place constraints on k_m and k_c based on the experimentally determined values of those present-day isotopic ratios. See Section 4.1 for discussion on why these scenarios were chosen.

3.1 Constant oxygen fugacity

First, I ran the model for a constant oxygen fugacity, where ΔIW remains constant at -2 log units. This corresponds to the present-day value for Fe content of the mantle (6.3 wt%) (Corgne et al., 2008). I plot these results in Figure 4. Here, k_c and k_m represent an average value of each parameter over all impacts, rather than an individual value for each impact. The regions that satisfy the present-day tungsten and lead constraints are referred to as the isotopic bounds for those systems respectively.

Each region bounded by the isotopic constraints is confined by a horizontal asymptote that corresponds to a lower bound of k_m and a vertical asymptote that corresponds to a lower bound of k_c. At τ_a = 25 Myr, the lead and tungsten isotopic constraints do not intersect, meaning there are no values of k_c and k_m that satisfy both the lead and tungsten constraints. Beginning with τ_a = 30 Myr, the isotopic bounds begin to intersect at minimum values of k_c = 0.57 and k_m = 0.46. As the timescale of accretion lengthens but the number of impactors remains constant, the isotopic constraints intersect at continuously smaller values of k_c as the lead bounds narrow and the vertical asymptote moves to lower values of k_c. In addition, with higher mean age of accretion, the horizontal asymptote of the lead bounds lowers significantly. At τ_a = 170 Myr, the lead and tungsten bounds do not intersect anymore. As the number of impactors increases, the horizontal k_m asymptotes of both the lead and the tungsten isotopic bounds decrease in value of k_m. For example, when $n_i = 10$, the horizontal asymptote for lead ranges from approximately k_m = 0.46 to 0.41.

3.2 Increasing oxygen fugacity

3.2.1 Case 1

In the first case for increasing oxygen fugacity, ΔIW increases from -4 to -2. This evolving oxygen fugacity represents an increase of 0.63 wt% Fe in the mantle to 6.3 wt% Fe in the mantle (Wade and Wood, 2005). The results, seen in Figure 5, are overall similar to results from the constant oxygen fugacity model. The isotopic bounds are confined by a horizontal asymptote that corresponds to a lower bound of k_m and a vertical asymptote that corresponds to a lower bound of k_c.

As was the case for a constant oxygen fugacity scenario, at τ_a = 25 Myr, the lead and tungsten isotopic bounds do not intersect. At τ_a = 30 Myr, the bounds first intersect at k_c = 0.46 and k_m = 0.46. In these early accretion scenarios, acceptable values of k_m and k_c are controlled by the tungsten constraints. The lead bounds overlap with the tungsten bounds at the horizontal asymptote for tungsten, so k_m is well constrained. With an increasing mean age of accretion, the vertical k_c asymptote moves to lower values of k_c, and the lead isotopic bounds narrow. An increasing number of impactors leads to the horizontal k_m asymptote moving to lower values of k_m. For $n_i = 10$, the horizontal asymptote for the tungsten bounds ranges from approximately k_m = 0.46 - 0.39. In later accretion scenarios, the region of overlap consists of high k_m values and low k_c values.When τ_a = 170 Myr, the lead and tungsten regions no longer intersect, and there are no values of k_c and k_m that satisfy isotopic conditions.

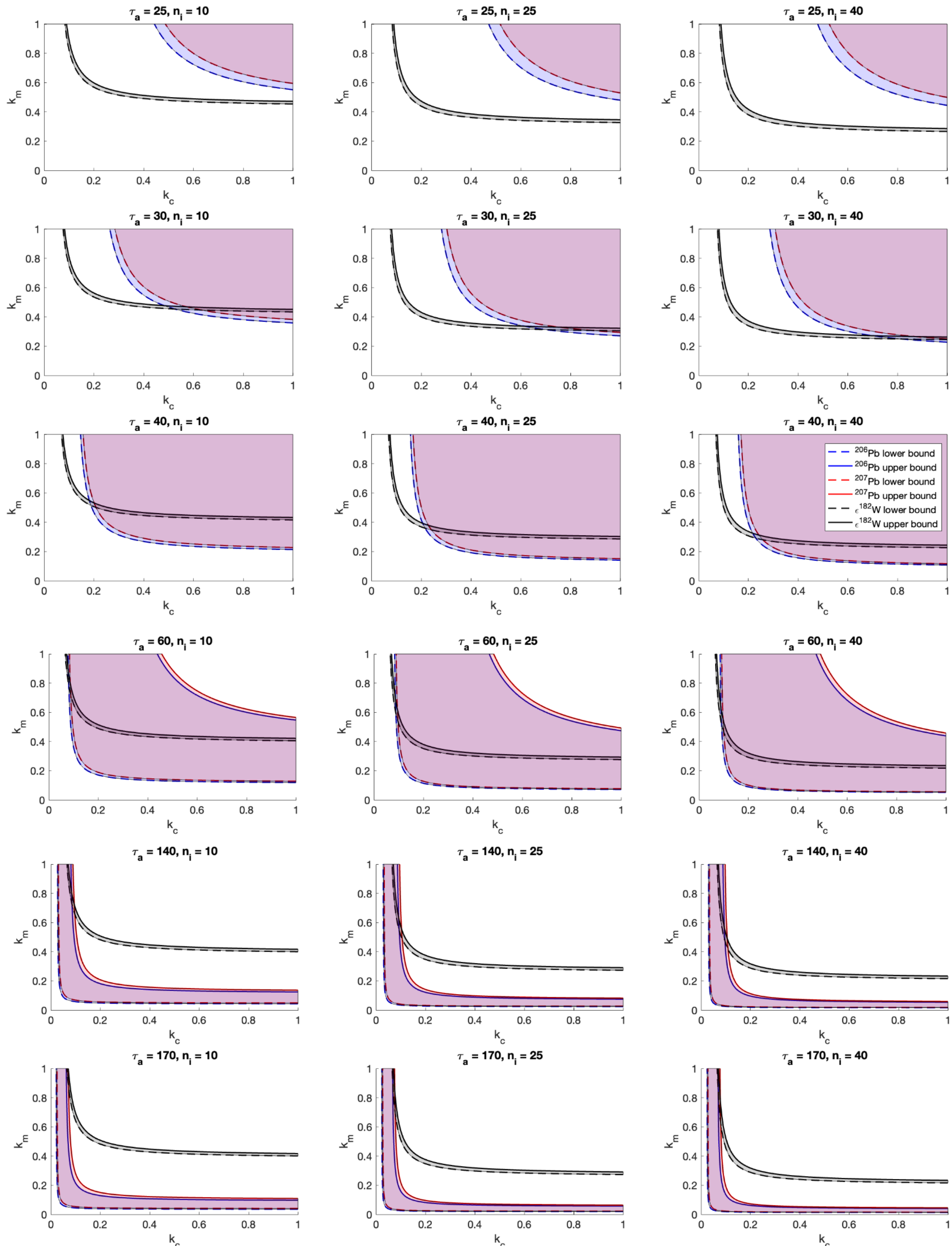

Figure 4. Core equilibration fraction vs. mantle equilibration fraction for 6 different τ_a (mean age of accretion) and 3 different n_i (number of impactors) when ΔIW = -2. The black lines represent the tungsten isotopic bounds, the blue the lead-206 bounds, and red the lead-207 bounds. Dashed lines are the lower bounds and solid lines are the upper bounds.

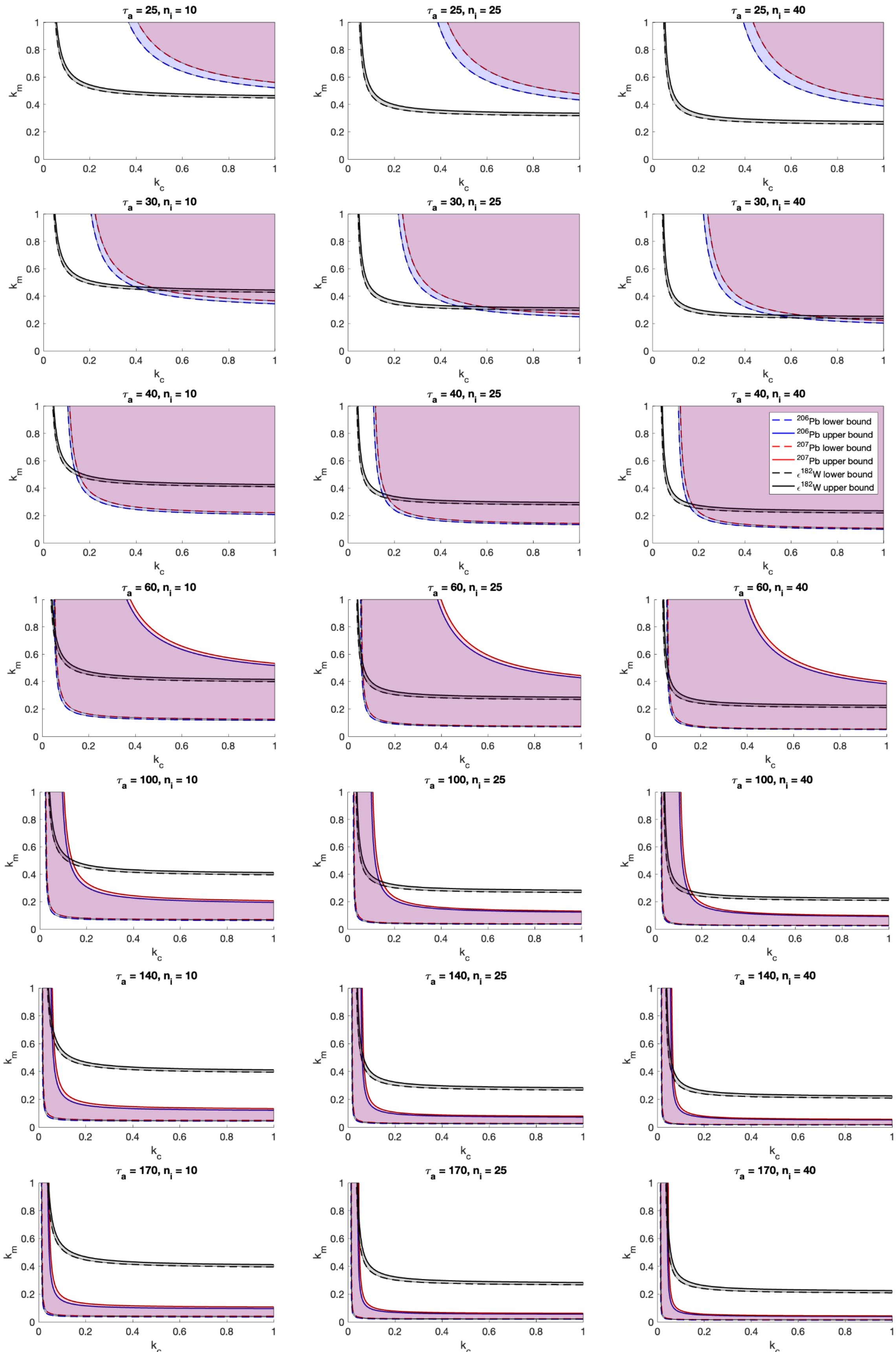

Figure 5. Core equilibration fraction vs. mantle equilibration fraction for 7 different τ_a (mean age of accretion) and 3 different n_i (number of impactors) when ΔIW increases from -4 to -2 in log units.

3.2.2 Case 2

In the second case for increasing oxygen fugacity, ΔIW increases from -4.5 to -1 in log units (Figure 6). This is approximately analogous to the oxygen fugacity conditions in equilibrium model of Rudge et al. (2010); we could not generate results that corresponded within the known experimental values of the present-day lead and tungsten isotopic ratios with the oxygen fugacity conditions in their disequilibrium model (see section 4.2). In contrast to the two aforementioned oxygen fugacity scenarios, an increase in ΔIW from -4.5 to -1 generates noticeable different results.

Under these oxygen fugacity conditions, the timescale of accretion is considerably narrowed in comparison to accretion under constant oxygen fugacity or under the previously mentioned regime of oxygen fugacity increase. The lead and tungsten isotopic bounds do not intersect until τ_a = 30 Myr; when τ_a = 25 Myr, only the lead isotopic bounds are visible on the plot. When τ_a = 30 Myr and n_i = 10, the lead and tungsten bounds first intersect at a higher value of k_c = 0.71 and k_m = 0.75. However, at τ_a = 30 Myr and n_i = 40, the tungsten and lead regions do not intersect. A higher number of impacts, in all accretion timescales, considerably narrows the region of acceptable k_c and k_m. As in the constant oxygen fugacity model and the Case 1 increasing oxygen fugacity model, increasing mean age of accretion lowers both the horizontal and vertical asymptotes of the lead bounds. The tungsten bounds, under these oxygen fugacity conditions, fall in a much higher range of k_c than in prior scenarios. The minimum k_c that satisfies the isotopic constraints of the model is k_c = 0.32, when τ_a = 80, n_i = 40, and k_m = 1. At τ_a = 100 Myr, the lead and tungsten bounds no longer intersect, and there are no values of k_c and k_m that satisfy all of the present-day isotope ratio constraints.

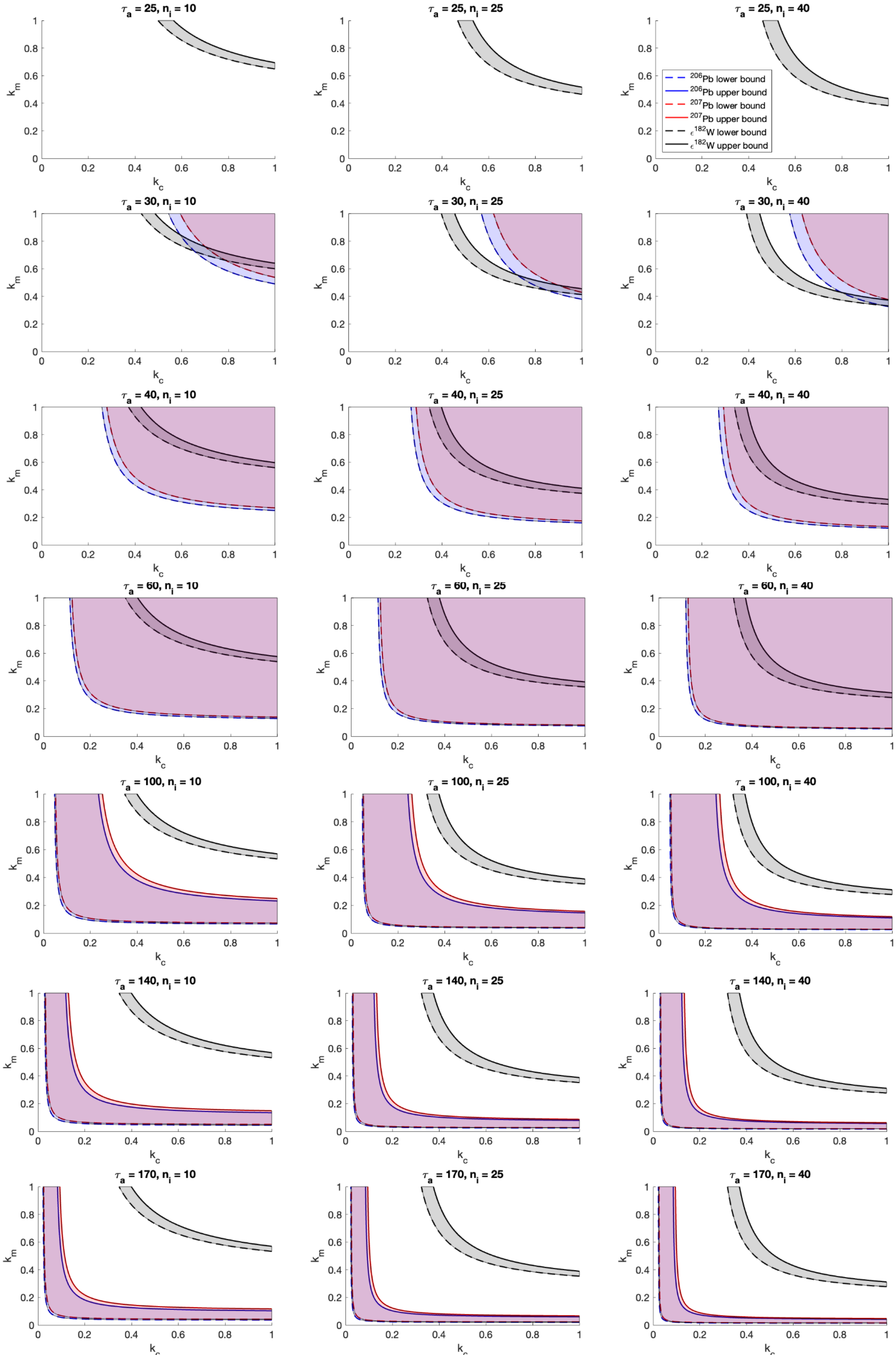

Figure 6. Core equilibration fraction vs. mantle equilibration fraction for 7 different τ_a (mean age of accretion) and 3 different n_i (number of impactors) when ΔIW = -4.5 to -1.

4. Discussion

In this section, I discuss the physical meaning of our results and discuss the sensitivity of the model to oxygen fugacity. I also compare our results to Rudge et al. (2010), a study that also built a geochemical model to constrain degree of core equilibration during accretion.

Mean age of accretion was likely confined between 25 Myr and 170 Myr. The earliest and latest mean ages in this broad range have the smallest range of values of k_c and k_m that fall within the lead and tungsten isotopic bounds. Because of the short-lived nature of the Hf–W radiogenic isotope system, the region bound by tungsten constraints is very narrow and thus acts as a major control on acceptable values of k_c and k_m (although it most affects k_m). In contrast, the U–Pb system most affects acceptable values of k_c and does not exert control over k_m. Generally, earlier accretion timescales result in a higher average k_c of impactors within the range of acceptable k_c values. Later accretion timescales result in lower average k_c of impactors, and mid-range accretion timescales (like τ_a = 60 Myr) do not constrain the k_c values much at all. The accretion timescale most affects the satisfaction of lead isotopic constraints; because the Hf–W system is extinct and hafnium-182 has a short half life, tungsten ratios are most useful tracking core formation in the first 60 Myr or so.

Meanwhile, the number of impacts most affects the tungsten constraints. As the number of impacts increases, the k_m bounds of the tungsten isotope system decrease, as well as the k_m bounds of the lead region. Average k_m is lower for a larger number of impacts; this is in part due to the accretion curve model, where each impactor (besides Theia of the lunar-forming impact) is the same size. This size is equal to 0.90 divided by the number of impactors, so with more impactors, their size decreases. Smaller impactors generate a smaller fraction of a magma ocean, since in comparison, the energy the impact generates is lower.

4.1 Oxygen fugacity

Core-mantle equilibration is extremely sensitive to the oxygen fugacity conditions of the model. Partitioning of elements between the mantle and the core during equilibration relies heavily on temperature, pressure, and oxygen fugacity. One popular theory posits that accretion began with reduced material and the later part of Earth accretion was dominated by highly oxidized material; thus the oxygen fugacity must have increased (Wanke, 1981). Observed mantle depletions in refractory elements are consistent with an oxygen fugacity increase of 2 log units during accretion. I chose an oxygen fugacity increase of $\Delta IW = -4$ to -2, but some studies say it could increase from $\Delta IW = -5$ to -3 or $\Delta IW = -3$ to -1. However, our model does not consider the conditions under which the embryos differentiate. If the impactors differentiate under highly reducing conditions, oxygen fugacity may not need to increase over the course of accretion. Wade and Wood (2005), though, claim this is physically impossible: if the bottom of the magma ocean must be at or below the liquidus, a fixed oxygen fugacity would require the sinking pieces of impactor core to stop equilibrating at only half of the depth of the magma ocean. Regardless, the results for both constant oxygen fugacity and an evolving oxygen fugacity from $\Delta IW = -4$ to -2 are quite similar, and provide roughly the same constraints on core-mantle equilibration fractions.

An approximate increase in oxygen fugacity from $\Delta IW = -4.5$ to -1 considerably narrows the constraints on core-mantle equilibration. The accretion timescales that produce acceptable results within the isotopic constraints are narrowed. This oxygen fugacity scenario, taken from the Rudge et al. (2010) penalty approach to trace element inversion, is not widely supported by the literature, and was used in this thesis to compare our results to the prior study. Most studies agree that the oxygen fugacity either increased two log units over the course of accretion or remained constant for the whole of accretion (Wade and Wood, 2005; Corgne et al., 2008). In comparison to the other two scenarios listed above, this scenario provides less constraint on equilibration fractions because the region of values that satisfy the present-day tungsten isotopic ratios is significantly wider.

4.2 Comparison with Rudge et al. (2010)

It is difficult to compare our results directly with Rudge et al. (2010), because their study only considered impactor cores equilibrating with a full magma ocean. To compare our geochemical model to the one in Rudge et al. (2010), I reproduced Figure 3a of that study with our model. Figure 7a shows Figure 3a from Rudge et al. (2010), while Figure 7b shows our reproduction of that figure using an increasing oxygen fugacity from ΔIW = -4.5 to -1. The two are similar enough that we can assume that our geochemical models are comparable and we can directly relate our results to theirs.

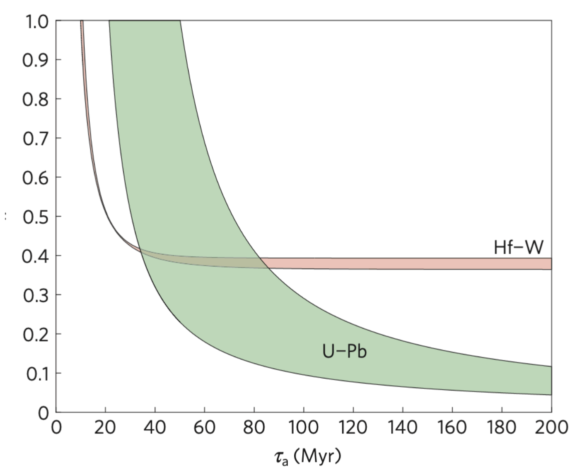

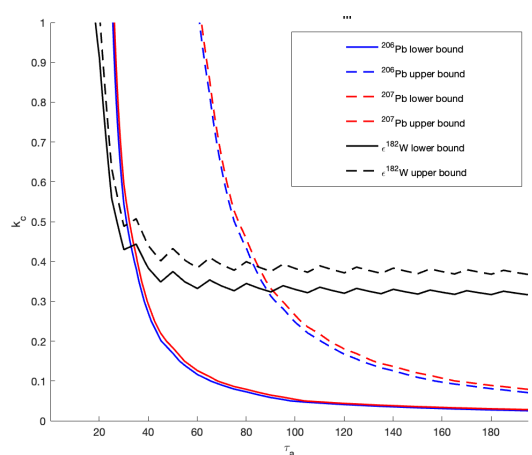

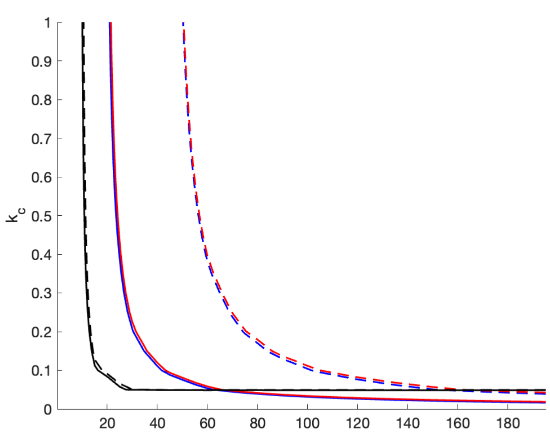

Figure 7. Core equilibration fraction as a function of τ_a. **a, upper left)** From Rudge et al. (2010), Figure 3b. **b, upper right)** Reproduction of a) using ΔIW_1 = -4.5 and ΔIW_2 = -1. **c, lower left)** Reproduction of a) using ΔIW_1 = -4 and ΔIW_2 = -2

I also reproduce that figure with an increasing oxygen fugacity from ΔIW = -4 to -2, seen in Figure 7c. These oxygen fugacity parameters drastically affect the values of k_c and τ_a that are compatible with the tungsten isotopic constraints. The intersection of the regions bound by isotopic constraints in the ΔIW = -4.5 to -1 scenario lies from approximately k_c = 0.36 - 0.5 and τ_a = 35 - 90 Myr. Because this figure sets k_m = 1, we can compare these to our results from Section 3.2.2 by looking at where k_m = 1 on Figure 6. From there, we can see that overlap between the isotopic bounds happens at k_m = 1 and k_c = 0.4 - 0.36. In contrast, when ΔIW increases from -4 to -2, the intersection of the tungsten and lead regions occurs at a much lower k_c of 0.05 and between τ_a = 65 - 160 Myr. Looking at Figure 5, the tungsten and lead regions do not overlap at k_m = 1 until τ_a > 60 Myr; even then, the tungsten constraints are extremely narrow and have a vertical asymptote of k_c = 0.05. This indicates that impactor cores barely equilibrated with the mantle before joining the Earth's core, and thus the Earth's core then must retain the chemical signature of the impactor cores.

We could not produce results that corresponded with the known isotopic constraints using the oxygen fugacity conditions from the disequilibrium model of Rudge et al. (2010). Their model uses a penalty function approach to trace element inversion to determine the values of P_0, ΔIW_1, and ΔIW_2 that best fit the observed present-day mantle depletion for moderately siderophile elements. For a disequilibrium model, where k_c = 0.42, they determined ΔIW_1 to be -2.62 and ΔIW_2 to be -0.57. When I use these parameters in the model, there are no results within both of the isotopic constraints; in fact, for all accretion scenarios investigated, there are no values of k_c or k_m that satisfy the tungsten isotopic constraints at all. Because the Rudge et al. (2010) model does not consider a varying k_m in its disequilibrium model, it is likely that the method used to obtain these values of oxygen fugacity also did not, and that could be a reason for these parameters being incompatible with our model. In addition, the initial oxygen fugacity is possibly too reduced to produce valid present-day isotopic ratios.

5. Conclusion

This study created a comprehensive model for Earth accretion with the aim of constraining core-mantle equilibration processes and understanding how accreting materials interact with a growing proto-Earth. We were able to discern the effect of accretion timescale and impactor size on core (k_c) and mantle (k_m) equilibration fractions, as well as illustrate the sensitivity of elemental partitioning and consequently equilibration to oxygen fugacity conditions.

To further unravel the process of Earth and terrestrial planet formation, we must add more parameters to our model and increase the complexity of our model. For example, the impactors in our model differentiate at the same time and, after, are left alone until they collide with the proto-Earth. A more realistic model would incorporate the embryos colliding with each other, affecting their own mantle and core compositions, before eventually impacting the Earth. In addition, the impactors are all the same size, and varying impactor size would affect the fraction of the mantle that is molten in the model. Due to the stochastic nature of these impacts, we could incorporate a Markov chain to further constrain k_c, k_m, and other parameters of Earth accretion. Our current analysis, while illuminating compared to past studies, could provide even narrower constraints on the processes of mixing and equilibration during planetary formation. This is particularly crucial in the context of terrestrial habitability, as it is probable that most life-essential elements and compounds on Earth were delivered to the planet during accretion.

Acknowledgements

I would like to thank everyone who has helped me in the development of this senior thesis throughout what has been a very difficult senior year. Thank you to my advisor, Professor Jun Korenaga, for introducing me to the world of geochemical modeling and lending me that copy of *The Practice of Programming* from your bookshelf in December. Thank you to my second reader, Assistant Professor Alan Rooney, for introducing me to isotope geochemistry (and *Speed* featuring Keanu Reeves). Thank you to Professor Maureen Long for being my biggest supporter during my time in the Yale Earth and Planetary Sciences Department. Thank you to my housemates (the “216-agers”) for forcing me to take a break and watch *The Bear* with them. Thank you to Brianna Fernandez, my best friend and geophysical partner-in-crime, for driving the literal and metaphorical getaway car in my many times of need. Most of all, thank you to my ancestors, who stewarded the lands of the very Earth I study and fought so that our people could survive. It was our culture and traditions that drove me to geology in the first place; *ᏩᏙ ᎠᏍ ᏙᏓᏓᎪᎲᎢ*.

References

Broadley, M. W., Bekaert, D. V., Piani, L., Füri, E., & Marty, B. (2022). Origin of life-forming volatile elements in the inner Solar System. *Nature*, *611*(7935), 245–255. https://doi.org/10.1038/s41586-022-05276-x

Corfu, F. (2013). A century of U-pb geochronology: The long quest towards concordance. In *Bulletin of the Geological Society of America* (Vol. 125, Issues 1–2). https://doi.org/10.1130/B30698.1

Corgne, A., Keshav, S., Wood, B. J., McDonough, W. F., & Fei, Y. (2008). Metal-silicate partitioning and constraints on core composition and oxygen fugacity during Earth accretion. *Geochimica et Cosmochimica Acta*, *72*(2). https://doi.org/10.1016/j.gca.2007.10.006

Deguen, R., Landeau, M., & Olson, P. (2014). Turbulent metal–silicate mixing, fragmentation, and equilibration in magma oceans. *Earth and Planetary Science Letters*, *391*, 274–287. https://doi.org/10.1016/J.EPSL.2014.02.007

Halliday, A. N. (2004). Mixing, volatile loss and compositional change during impact-driven accretion of the Earth. *Nature*, *427*(6974), 505–509. https://doi.org/10.1038/nature02275

Halliday, A. N., & Canup, R. M. (2022). The accretion of planet Earth. *Nature Reviews Earth & Environment*, *4*(1), 19–35. https://doi.org/10.1038/s43017-022-00370-0

Kleine, T., Touboul, M., Bourdon, B., Nimmo, F., Mezger, K., Palme, H., Jacobsen, S. B., Yin, Q. Z., & Halliday, A. N. (2009). Hf–W chronology of the accretion and early evolution of asteroids and terrestrial planets. *Geochimica et Cosmochimica Acta*, *73*(17), 5150–5188. https://doi.org/10.1016/J.GCA.2008.11.047

Lee, D.-C., & Halliday, A. N. (1995). Hafnium–tungsten chronometry and the timing of terrestrial core formation. *Nature*, *378*(6559), 771–774. https://doi.org/10.1038/378771a0

Morbidelli, A., Lunine, J. I., O'Brien, D. P., Raymond, S. N., & Walsh, K. J. (2012). Building terrestrial planets. In *Annual Review of Earth and Planetary Sciences* (Vol. 40). https://doi.org/10.1146/annurev-earth-042711-105319

Patterson, C. (1956). Age of meteorites and the earth. *Geochimica et Cosmochimica Acta*, *10*(4), 230–237. https://doi.org/10.1016/0016-7037(56)90036-9

Peslier, A. H., Schönbächler, M., Busemann, H., & Karato, S.-I. (2017). Water in the Earth's Interior: Distribution and Origin. *Space Science Reviews*, *212*(1–2), 743–810. https://doi.org/10.1007/s11214-017-0387-z

Rubie, D. C., Nimmo, F., & Melosh, H. J. (2015). Formation of the Earth's Core. In *Treatise on Geophysics: Second Edition* (Vol. 9). https://doi.org/10.1016/B978-0-444-53802-4.00154-8

Rudge, J. F., Kleine, T., & Bourdon, B. (2010). Broad bounds on Earth's accretion and core formation constrained by geochemical models. *Nature Geoscience*, *3*(6). https://doi.org/10.1038/ngeo872

Wade, J., & Wood, B. J. (2005). Core formation and the oxidation state of the Earth. *Earth and Planetary Science Letters*, *236*(1–2), 78–95. https://doi.org/10.1016/J.EPSL.2005.05.017

Wanke, H., & Gold, T. (1981). Constitution of Terrestrial Planets [and Discussion]. *Phil. Trans. R. Soc. Lond.*, *303*.

Yin, Q., & Jacobsen, S. B. (2006). Does U–Pb date Earth's core formation? *Nature*, *444*(7115), E1–E1. https://doi.org/10.1038/nature05358